

# Measurement of $\pi^0\pi^{+/-}$ photoproduction off the deuteron and dbutanol targets

Debdeep Ghosal<sup>1,\*</sup>  
 on behalf of A2 Collaboration

<sup>1</sup>University of Basel (Basel, CH)

**Abstract.** Recent experiments using the Crystal Ball/TAPS setup at the MAMI accelerator in Mainz, Germany continue to study the properties and the excitation spectrum of the nucleon with meson photoproduction. Electromagnetic excitations of the proton and neutron are essential for understanding their isospin decomposition. The electromagnetic coupling of photons to protons is different than that of neutrons in certain states. Cross-section data alone is not sufficient for separating resonances, whereas polarization observables play a crucial role being essential in disentangling the contributing resonant and non-resonant amplitudes. Preliminary results of the polarization observable  $E$  of double  $\pi$  production measured with a polarized solid deuterated Butanol target are shown with comparison to predictions of recent analyses.

## 1 Introduction

Quark models describe the behavior of quarks in nucleons at medium energies. Meson photoproduction allows to investigate the excited states (resonances) of nucleons. Unfortunately, many states are overlapping and cannot be easily differentiated from each other and many have been predicted, but not yet detected [1]. The states that have not yet been observed could be missing because they have not been seen experimentally until now or do not exist at all. Most earlier experiments were performed with pion beams and some resonances might couple less strongly to pions and couple more strongly to rare channels and have circumvented detection. Most results still arise from experiments on the proton, which does not allow for as much information regarding the isospin structure of the electromagnetic transitions. Therefore, advances in experiments on the neutron can provide an integral piece to the understanding of the nucleon spectrum [2]. Unfortunately, it is not possible to perform measurements on the free neutron, but a deuterated butanol target has allowed for the possibility to study spin effects with quasi-free neutrons.

We have preliminary results for the contribution of different channels with proton targets. Final results need of course a more profound analysis including interference effects etc. From the outcomes of total absorption experiment [3], there was discussion whether there is a significant contribution from  $D_{13} \rightarrow N\rho$ , because due to the predicted in-medium modifications of the  $\rho$  this could modify the  $D_{13}$  shape. One of the motivations for the present experiments with proton and deuteron targets is the extraction of a much more precise  $D_{13} \rightarrow N\rho$  branching ratio for those two targets.

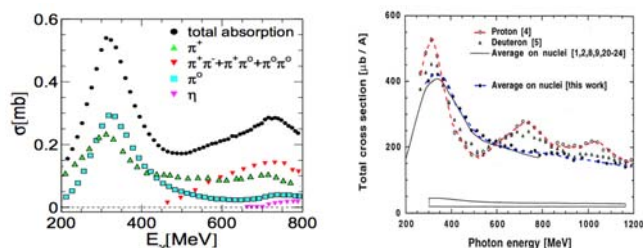


Figure 1: In the above left figure, much of the bump in the second resonance region is due to double pion production. The right figure above is also related to an old problem seen in total photoabsorption where the second resonance bump is completely suppressed for heavier nuclei [3].

For years, cross section data has been used to learn about the nucleon spectrum. However, cross section data alone is not enough to distinguish the broad overlapping resonances. Polarization observables can provide understanding of these overlapping resonances by discovering more information about the complex helicity amplitudes, which describe the interaction between photon beams and nucleons. These amplitudes are fully determined when a complete set of measurements is performed and give rise to the cross section, complemented by polarization observables including beam, target, and recoil asymmetries. Here the observable  $E$  (longitudinally polarized target and circularly polarized photon beam) will be discussed.

The relationship between the cross section and polarization observable  $E$  can be written in terms of the helicity of beam and target as follows:

\*e-mail: [debdeep.ghosal@unibas.ch](mailto:debdeep.ghosal@unibas.ch)

$$E_{version1} = \frac{\sigma_{1/2} - \sigma_{3/2}}{\sigma_{1/2} + \sigma_{3/2}} = \frac{\sigma_{diff}}{\sigma_{sum}} \quad (1)$$

$$E_{version2} = \frac{\sigma_{diff}}{2\sigma_{impol.}} \quad (2)$$

where  $\sigma_{1/2}$  is the cross section of events when beam and target polarizations are anti-parallel;  $\sigma_{3/2}$  is the cross section of events with when they are parallel.

## 2 Experimental Setup

The measurements were performed at the MAMI-C accelerator in Mainz, Germany [4]. A pictorial diagram of the main experimental setup has been shown below. A longitudinally polarized electron beam of energy 1557 MeV and polarization degree of 80% is delivered into the A2 experimental Hall. Circularly polarized photons are produced from a radiator and energy tagged using the Glasgow-Mainz photon tagger [6] with energies between 470 and 1450 MeV. The targets consists of a deuterated butanol material (dButanol) cooled to a low temperature with the deuterons either transversally or longitudinally polarized up to 80%. The target is surrounded by a cylindrical particle identification detector (PID) made up of 24 plastic scintillator strips that each cover  $15^\circ$  in the azimuthal angle. The PID is then surrounded by a multi-wire proportional chamber (MWPC) and the MWPC is surrounded by the spherical Crystal Ball (CB) calorimeter [6]. The CB consists of 672 NaI(Tl) crystals and covers  $20^\circ$  to  $160^\circ$  in the polar angle. In the forward direction, a hexagonal two arm photon spectrometer (TAPS) built from 72  $PbWO_4$  (two innermost rings) and 366  $BaF_2$  crystals (remaining rings) is present. A veto wall present in front of TAPS is used for particle identification. The combination of the CB and TAPS provides an almost  $4\pi$  acceptance in the center of mass frame with a high angular and energy resolution.

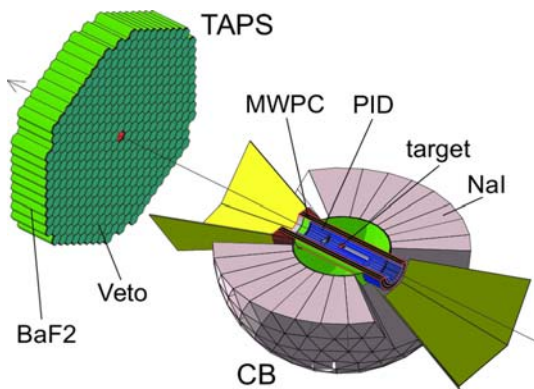


Figure 2: Schematic diagram of the experimental setup [5].

## 3 Analysis and Results

### 3.1 Event selection for the two amplitudes

Using information from the detectors, events are collected and then selected based on the number of charged or neutral hits. Neutral mesons are identified via a  $\chi^2$  test, which

tries to find the best combination of photon clusters for the meson invariant mass. To eliminate accidental coincident tagger photons, coincidence time cuts are applied and random background subtraction was performed. To separate the background from the signal, kinematic cuts were applied for each  $W$  and  $\cos\theta$  bin.

The analysis of  $\gamma p(n) \rightarrow \pi^0 \pi^+ n(n)$  requires the decay photons of the  $\pi^0$  meson to be detected as well as the  $\pi^+$  and the recoil neutron. Therefore, all events with 3 neutral clusters and 1 charged cluster are selected. A dE-E analysis was used to identify the charged pion [7]. The main source of background in this reaction comes from the following reaction that has the same final state:  $\gamma p(n) \rightarrow \eta \pi^+ n$

The analysis of  $\gamma n(p) \rightarrow \pi^0 \pi^- p(p)$  requires the decay photons of the  $\pi^0$  meson to be detected as well as the  $\pi^-$  and the recoil proton. Therefore, all events with 2 neutral clusters and 2 charged clusters are selected [7].

### 3.2 Polarization observable

A real photon can be either circularly or linearly polarised. Circularly polarised photons consists of two plane waves that have the same amplitude, but have a  $90^\circ$  difference in phase. For linearly polarised photons, this electric field vector is composed of only one plane wave. The target (such as proton or neutron) can be polarised in three different directions ( $x, y, z$ ) as well as the recoil (proton or neutron) in  $x', y', z'$ . Thus, in total,  $2 \times 3 \times 3 = 18$  double polarisation observables are theoretically possible. However, this number is reduced to only 12 observables since some combinations do not yield additional information. They can be divided into three groups as per the table below among which this paper is interested in  $E$  only.

Table 1: Double Polarization observables can be divided into three groups [8].

Beam-Target	Beam-Recoil	Target-Recoil
$G, H, E, F$	$O_x, O_z, C_x C_z$	$T_x, T_z, L_x, L_z$

Different versions were used to extract the beam asymmetry  $E$ . Version 1 refers to where a normalization with twice of the unpolarized cross section  $\sigma_0$  is used, which was measured with a liquid deuterium target, and does not need to utilize carbon background subtraction since the background is canceled in the difference of the two helicity states ( $\sigma_\Delta = \sigma_{1/2} - \sigma_{3/2}$ ). Version 2 refers to the normalization of the numerator using the sum of the two spin configurations ( $\sigma_\Sigma = \sigma_{1/2} + \sigma_{3/2}$ ) [9]. Here, the background from unpolarized carbon and oxygen nuclei inside the target have to be subtracted, allowing for events only on polarized protons and neutrons.

Preliminary results regarding comparison plots of total cross sections in terms of  $E_\gamma$ (photon energy) and  $W$ (center of mass energy) for dButanol targets are shown in Fig 4 and Fig. 5. Here only one version(in terms of  $E$ -observable) to calculate the total cross sections have been presented both in terms of direct and carbon subtracted

Table 2: Overview of different versions used to extract E asymmetry

version	E
1	$\frac{\sigma_{1/2} - \sigma_{3/2}}{2\sigma_0}$
2	$\frac{\sigma_{1/2} - \sigma_{3/2}}{\sigma_{1/2} + \sigma_{3/2}}$

Table 3: Overview of different versions used to extract two helicity state cross section components; where,  $\sigma_\Sigma = \sigma_{1/2} + \sigma_{3/2}$  and  $\sigma_\Delta = \sigma_{1/2} - \sigma_{3/2}$

version	$\sigma_{1/2}$	$\sigma_{3/2}$
1	$\frac{\sigma_0(1 + E)}{2}$	$\frac{\sigma_0(1 - E)}{2}$
2	$\frac{\sigma_\Sigma + \sigma_\Delta}{2}$	$\frac{\sigma_\Sigma - \sigma_\Delta}{2}$

method. Before that, efficiency comparison of the two interested channels has been presented below.

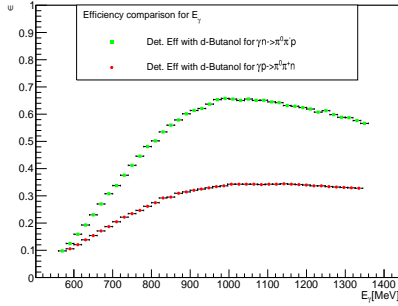


Figure 3: Detection efficiency comparison for the channels  $\gamma p \rightarrow \pi^0 \pi^+ n$  (red dots) and  $\gamma n \rightarrow \pi^0 \pi^- p$  (green dots) are shown above. It also indicates the higher efficiency for proton detection than that for the channel with neutron in final state.

### 3.3 E observable: Carbon subtraction method (Version-1)

For the determination of the carbon background dedicated beam-times were carried out, with the same experimental conditions as for the dButanol, but with a carbon target of identical density. For a proper background subtraction, the relative contributions of carbon and oxygen nuclei to the dButanol, also called dilution factor, has to be determined. This was done by comparing missing mass distributions of dButanol data, carbon data and deuterium data. If the individual data sets are properly normalized, the spectra of carbon and deuterium should add up to the dButanol. Missing mass distributions are especially suited for this comparison, as contributions from different nuclei are well separated, due to different Fermi momenta [7].

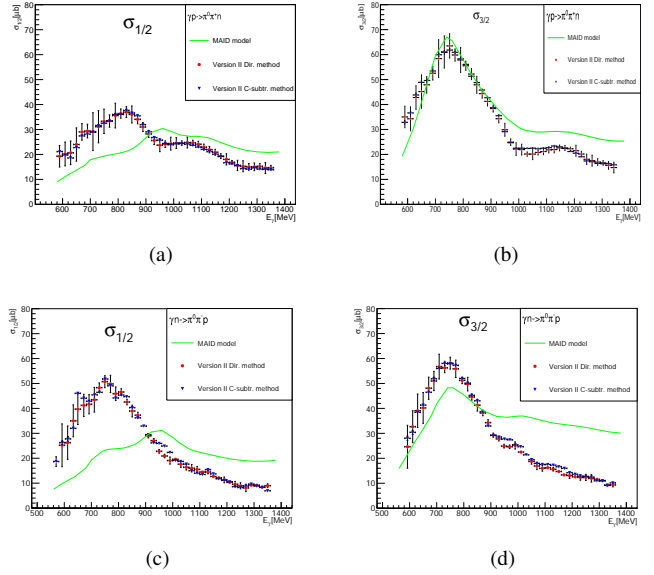


Figure 4: Total cross section comparison in terms of photon energy for  $\gamma p \rightarrow \pi^0 \pi^+ n$  (upper row) and  $\gamma n \rightarrow \pi^0 \pi^- p$  (bottom row). Different colored symbols in each case represent the cross sections determined with the direct and carbon subtracted method with both of the aforementioned versions, and the green line shape corresponds to that predicted by MAID model [10].

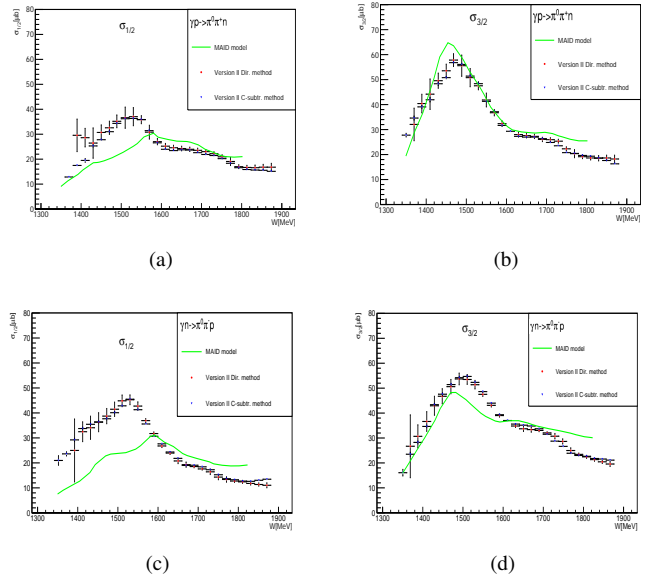


Figure 5: Total cross section comparison in terms of center of mass energy for  $\gamma p \rightarrow \pi^0 \pi^+ n$  (upper row) and  $\gamma n \rightarrow \pi^0 \pi^- p$  (bottom row). Different colored symbols in each case represent the cross sections determined with the direct and carbon subtracted method with both of the aforementioned versions, and the green line shape corresponds to that predicted by MAID model [10].

Preliminary results of  $E$  observable for  $\gamma p \rightarrow \pi^0 \pi^+ n$  and  $\gamma n \rightarrow \pi^0 \pi^- p$  channels both in terms of photon energy and center of mass energy are shown in Fig. 6.

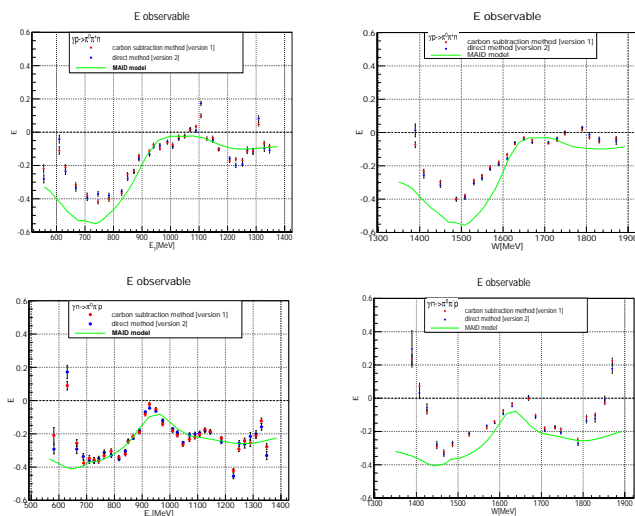


Figure 6:  $E$ -observable plots in terms of  $E_\gamma$  (photon energy) and  $W$  (center of mass energy) for  $\gamma p \rightarrow \pi^0 \pi^+ n$  (upper row) and for  $\gamma n \rightarrow \pi^0 \pi^- p$  (bottom row); Red dots are for the method with carbon subtraction and the Blue dots correspond to the direct method; and the green lineshape corresponds to that of MAID model prediction [11].

#### 4 Conclusion and Outlook

For two of these interested channels, there is significant non-vanishing  $E$ -observable asymmetry for both in terms of photon energy and center of mass energy. Extracted

results from the two different methods (version-1 and version-2) agree mostly with each other. The comparative study with the MAID model prediction is also quite satisfactory for the  $E$  asymmetry plots and fair for the helicity state cross section plots. Further investigation on background subtraction is under process for the final results. Data from further beamtimes with dButanol target is also being analyzed.

#### Acknowledgement

All of the results presented here have been obtained inside A2 collaboration at the Mainz MAMI accelerator. The support from Swiss National Fund (SNF) is kindly acknowledged.

#### References

- [1] R.G. Edwards *et al.*, Phys. Rev. **D84**, 074508 (2011)
- [2] [https://jazz.physik.unibas.ch/site/talks/krusche\\_dnp08.pdf](https://jazz.physik.unibas.ch/site/talks/krusche_dnp08.pdf)
- [3] F. Zehr and B. Krusche *et al.*, Eur. Phys. J. **A48(7)**, 98 (2012)
- [4] K. H. Kaiser *et al.*, NIM **A593**, 159 (2008)
- [5] [https://indico.cern.ch/event/739938/contributions/3411611/attachments/1859839/3056160/NSTAR\\_dghosal.pdf](https://indico.cern.ch/event/739938/contributions/3411611/attachments/1859839/3056160/NSTAR_dghosal.pdf)
- [6] J. C. George *et al.*, Eur. Phys. J. **A37**, 129 (2008)
- [7] [https://edoc.unibas.ch/55107/1/thesis\\_kaeser\\_2017.pdf](https://edoc.unibas.ch/55107/1/thesis_kaeser_2017.pdf)
- [8] [https://edoc.unibas.ch/39089/1/Lilian\\_Witthauer.pdf](https://edoc.unibas.ch/39089/1/Lilian_Witthauer.pdf)
- [9] [https://www.epj-conferences.org/articles/epjconf/pdf/2016/25/epjconf\\_meson2016\\_03009.pdf](https://www.epj-conferences.org/articles/epjconf/pdf/2016/25/epjconf_meson2016_03009.pdf)
- [10] <https://maid.kph.uni-mainz.de/twopion/>
- [11] <https://maid.kph.uni-mainz.de/maid2007/polariz.html>